Dynamics and Stability of Systems Vol. 4 Nos. 3 & 4 1989

Resonance in a high-speed flexible-arm robot

M. F. Golnaraghi
Department of Mechanical Engineering, University of Waterloo, Waterloo, Ontario, Canada

F. C. Moon
Sibley School of Mechanical and Aerospace Engineering, Cornell University, Ithaca, New York, USA

and R. H. Rand
Department of Theoretical and Applied Mechanics, Cornell University, Ithaca, New York, USA

Abstract

In this paper we consider the effects of nonlinearities due to Coriolis and centripetal forces on the motion of a multi-degree-of-freedom high-speed flexible-arm robot. We perform experimental investigations on a robot arm as well as analytical investigations on a mathematical model of the experimental apparatus. The two-variable expansion-perturbation method is used to describe the motions at internal and forced resonances. The perturbation solutions show the existence of a jump phenomenon and 'saturation' when both forced resonance as well as when 2:1 internal resonance occur. This phenomenon is also observed in the experiments, thus proving the accuracy of the perturbation solution.

Introduction

Multi-degree-of-freedom nonlinear systems have been the subject of numerous recent investigations (for example (Storti and Rand, 1982; Keith and Rand, 1984; Chatraborty and Rand, 1989; Golnaraghi, 1988)). Robotic mechanisms are a direct application of these studies. The complicated nature of these systems has produced limited progress in their design and control. Robotic devices are usually modelled by many coupled, nonlinear differential equations which are impossible to solve exactly. Understanding the nonlinear behaviour of these equations would contribute to the fabrication of a new generation of robots which are lightweight, highly mobile, and capable of carrying heavy payloads. Clearly, these characteristics would imply larger amplitudes of oscillation of the robot arm due to the effects of arm rotation and arm flexibility.

The kinematic nonlinear forces can, in general, be categorized as quadratic nonlinearities, and their appearance in n-degree-of-freedom systems can cause strong coupling between the various modes. For example, for a two-degree-of-

freedom system, the equations of motion take the form

$$\left.\begin{aligned} \ddot{x}_1 + \omega_1^2 x_1 &= -\gamma_1 \dot{x}_1 + 2\dot{x}_1\dot{x}_2 + F_1 \cos(\Omega_1 t + \tau_1), \\ \ddot{x}_2 + \omega_2^2 x_2 &= -\gamma_2 \dot{x}_2 + \dot{x}_1^2 + F_2 \cos(\Omega_2 t + \tau_2), \end{aligned}\right\} \tag{1}$$

where $2\dot{x}_1\dot{x}_2$ and $\dot{x}_1^2$ are Coriolis and centripetal nonlinearities, respectively.

If the natural frequencies for an n-degree-of-freedom system are denoted by $\omega_1, \omega_2, \ldots, \omega_n$, an 'internal resonance' will occur when $\sum_{i=1}^{n} a_i\omega_i = 0$, where the a_i are positive or negative integers including zero; that is $a_i \in \mathbb{Z}$. Moreover, if a periodic excitation with frequency Ω acts on a multi-degree-of-freedom nonlinear system, then resonances will occur when $p\Omega = \sum_{i=1}^{n} b_i\omega_i$, where $p, b_i \in \mathbb{Z}$.

In the case of two-degree-of-freedom systems, forced and internal resonances have been studied recently by Stupnicka (1969, 1978, 1980). Studies by Van Dooren (1971, 1972, 1973) reveal that combination tones could exist in two-degree-of-freedom systems containing two input frequencies Ω_1 and Ω_2. The resonances in these studies were of the form $\omega_n \simeq \Omega_2 \pm \Omega_1$, with ω_n as one of the natural frequencies. For a two-degree-of-freedom system having quadratic nonlinearities in which $\omega_2 \simeq 2\omega_1$, the amplitude of the mode being directly excited would have an upper bound when $\Omega \simeq \omega_2$. This phenomenon is called 'saturation' which is unique to systems with quadratic nonlinearities and has been studied by Nayfeh and Mook (1979) and Haddow *et al.* (1984).

In this paper we perform an analytical and experimental investigation of the dynamics of a high-speed two-degree-of-freedom flexible-arm robotic device, shown in Fig. 1. The arm is subjected to translational and rotational periodic inputs. Because of the complexity of the actual system, a simple mathematical model is developed to ease the theoretical and numerical studies. The second-order, nonlinear, coupled, ordinary differential equations possess quadratic nonlinearities. The equations of motion are non-dimensionalized and scaled.

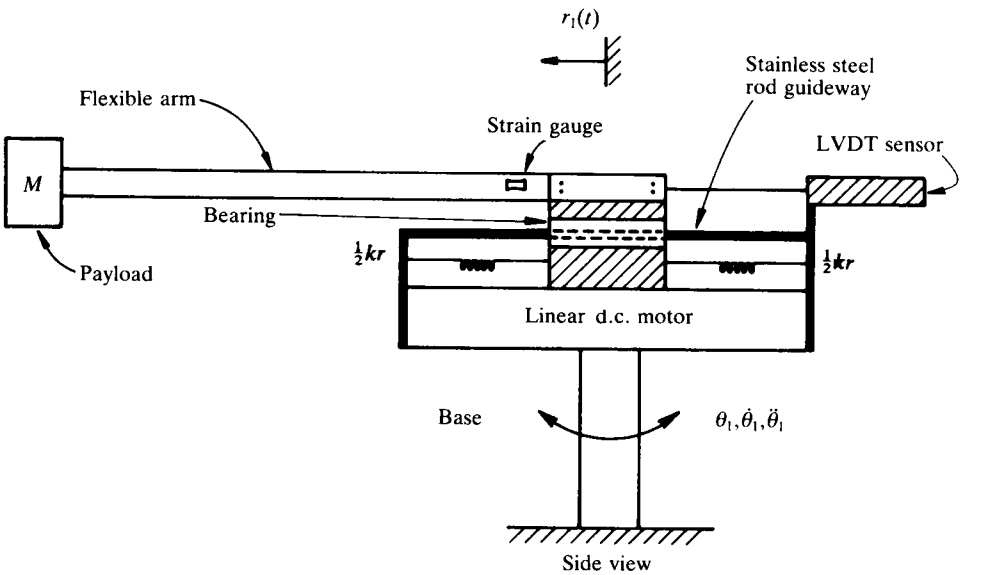

Fig. 1. Experimental apparatus showing a two-degree-of-freedom flexible-arm robot

The two-variable expansion-perturbation method is used in analysing the stability of the system for resonant and non-resonant cases. Consequently, all the possible resonances to the first order of approximation are located, and a study of the case of forced resonances is presented. Comparison of the experimental results with the perturbation solution indicates that the two-variable expansion method provides a good approximation of the motion of the system when the amplitudes of oscillation are sufficiently small.

Description of the mathematical model

The robotic mechanism shown in Fig. 1 consists of an oscillating base and a flexible arm which has a translational motion. The gripper and the mass of the payload are simply replaced by a single mass M. This system can be modelled as a simple sliding-pendulum mechanism as shown in Fig. 2. The (X_0, Y_0, Z_0)-reference frame is stationary and is centred at the point P. The (x_1, y_1, z_1)-coordinate set at the point P is rotating relative to the base. Mass M_1 represents the mass of the d.c. motor magnet assembly. Mass M_2 is the mass of the body transported by the arm, as well as the effective mass of the flexible arm r_2. The flexibility of the arm is taken into account by using a torsional spring with spring

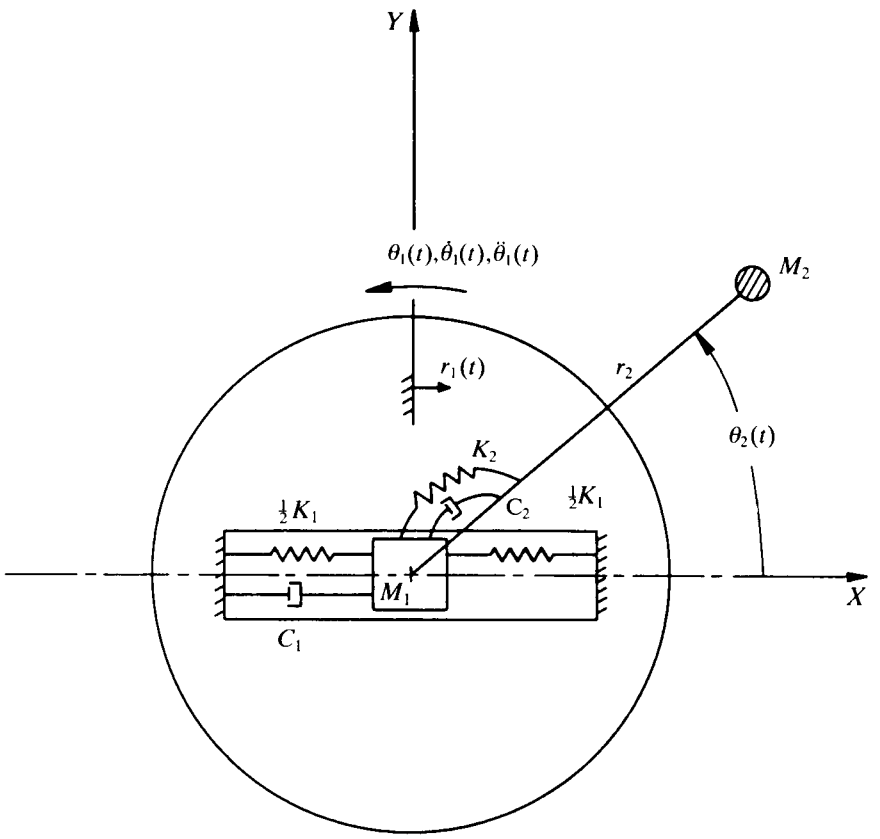

Fig. 2. A simple dynamical model representing the flexible-arm device

stiffness K_2. The stiffness of the springs used to mechanically centre the position of mass M_1 is represented by K_1, and C_1 and C_2 are the translational and rotational damping coefficients of the system, respectively.

Derivation of the equations of motion

The equations of motion of the mechanism shown in Fig. 2 were obtained by using Lagrangian dynamics. These equations were derived analytically both by hand and by use of the symbolic manipulation system MACSYMA, using a computer program which generates the dynamical equations of robotic mechanisms, developed by Golnaraghi *et al.* (1985).

For the model developed for the two-degree-of-freedom robotic device, the kinematics are easily derived using vector algebra. Considering Fig. 2 we define

$$\mathbf{r}_{m_1} = \mathbf{r}_1, \qquad \mathbf{r}_{m_2} = \mathbf{r}_1 + \mathbf{r}_2 \tag{2}$$

as the vectors describing the positions of masses M_1 and M_2. Thus, the velocities of M_1 and M_2 are

$$\left.\begin{aligned} \dot{\mathbf{r}}_{m_1} &= \dot{r}_1\hat{\imath} + r_1\dot{\theta}_1\hat{\jmath}, \\ \dot{\mathbf{r}}_{m_2} &= (\dot{r}_1 - r_2(\dot{\theta}_1 + \dot{\theta}_2)\sin(\theta_2))\hat{\imath} + (r_1\dot{\theta}_1 + r_2(\dot{\theta}_1 + \dot{\theta}_2)\cos(\theta_2))\hat{\jmath}. \end{aligned}\right\} \tag{3}$$

where $\hat{\imath}, \hat{\jmath}$ and $\hat{k}$ are the unit vectors of the (X, Y, Z)-coordinate frame. Hence, the kinetic energy of the system can then be written as

$$\begin{aligned} \mathrm{KE} &= \tfrac{1}{2}m_1\dot{\mathbf{r}}_{m_1}\cdot\dot{\mathbf{r}}_{m_1} + \tfrac{1}{2}m_2\dot{\mathbf{r}}_{m_2}\cdot\dot{\mathbf{r}}_{m_2} \\ &= \tfrac{1}{2}m_1(\dot{r}_1^2 + r_1^2\dot{\theta}_1^2) + \tfrac{1}{2}m_2(\dot{r}_1^2 + r_1^2\dot{\theta}_1^2 + r_2^2(\dot{\theta}_1 + \dot{\theta}_2)^2 \\ &\quad + 2\dot{r}_1 r_2(-(\dot{\theta}_2 + \dot{\theta}_1)\sin(\theta_2)) + 2r_1 r_2((\dot{\theta}_1\dot{\theta}_2 + \dot{\theta}_1^2)\cos(\theta_2))). \end{aligned} \tag{4}$$

The potential energy of the system simply involves that of the springs K_1 and K_2, and can be expressed as

$$\mathrm{PE} = \tfrac{1}{2}K_1 r_1^2 + \tfrac{1}{2}K_2\theta_2^2. \tag{5}$$

Lagrange's equations of motion of the system are

$$\left.\begin{aligned} &(m_1 + m_2)\ddot{r}_1 + C_1\dot{r}_1 + K_1 r_1 - m_2 r_2(\ddot{\theta}_2\sin(\theta_2) + \dot{\theta}_2^2\cos(\theta_2)) \\ &\quad - m_2 r_2(\ddot{\theta}_1(t)\sin(\theta_2) + \dot{\theta}_1^2(t)\cos(\theta_2) + 2\dot{\theta}_1(t)\dot{\theta}_2\cos(\theta_2)) \\ &\qquad -(m_1 + m_2)r_1\dot{\theta}_1^2(t) = F_r(t), \\ &m_2 r_2^2\ddot{\theta}_2 + C_2\dot{\theta}_2 + K_2\theta_2 - m_2 r_2 r_1\sin(\theta_2) \\ &\quad + m_2 r_2 r_1(\ddot{\theta}_1(t)\cos(\theta_2) + \dot{\theta}_1^2(t)\sin(\theta_2)) + 2m_2 r_2\dot{\theta}_1(t)\dot{r}_1\cos(\theta_2) \\ &\qquad = -m_2 r_2^2\ddot{\theta}_1(t), \end{aligned}\right\} \tag{6}$$

where

$$F_r(t) = A\cos(\Omega_r t), \qquad \theta_1 = F_2\sin(\Omega_\theta t). \tag{7}$$

Note that θ_2 and r_1 are generalized coordinates (dependent variables) while θ_1 and r_2 are given.

At this point it should be mentioned that the nonlinear terms in $(6)_{1,2}$ are due to the effect of rotation on the geometry of the structure. Note that the unforced equations of motion have a stable equilibrium position at ($r_1 = 0$, $\dot{r}_1 = 0$, $\theta_2 = 0$, $\dot{\theta}_2 = 0$). In the approximate solution which follows we shall replace the nonlinear trigonometric terms in $(6)_{1,2}$ by truncated Taylor expansions about this equilibrium.

Non-dimensional and scaled equations of motion

In order to generalize the problem, the equations of motion $(6)_{1,2}$ are non-dimensionalized. The non-dimensional equations take the form

$$\left.\begin{aligned} &\ddot{\rho}_1 + \gamma_1\dot{\rho}_1 + \omega_1^2\rho_1 - m(\ddot{\theta}_2 \sin(\theta_2) + \dot{\theta}_2^2 \cos(\theta_2)) \\ &\quad - m(\ddot{\theta}_1 \sin(\theta_2) + 2\dot{\theta}_1\dot{\theta}_2 \cos(\theta_2) + \dot{\theta}_1^2 \cos(\theta_2)) - \rho_1\dot{\theta}_1^2 \\ &\qquad = f_1\omega_1^2 \cos(\Omega_1\tau), \\ &\ddot{\theta}_2 + \gamma_2\dot{\theta}_2 + \omega_2^2\theta_2 - \ddot{\rho}_1 \sin(\theta_2) \\ &\quad + \rho_1(\ddot{\theta}_1 \cos(\theta_2) + \dot{\theta}_1^2 \sin(\theta_2)) + 2\dot{\theta}_1\dot{\rho}_1 \cos(\theta_2) = -\ddot{\theta}_1, \end{aligned}\right\} \tag{8}$$

where dots represent differentiation with respect to the non-dimensional time τ, defined as

$$\tau = \Omega t. \tag{9}$$

In (9), Ω is the non-dimensionalizing frequency. The non-dimensional variables are ρ_1 and θ_2, with

$$\rho_1 = r_1/r_2. \tag{10}$$

The non-dimensional mass is defined as

$$m = \frac{m_2}{m_1 + m_2}. \tag{11}$$

The natural frequencies of the uncoupled, unforced linear system are

$$\omega_1 = \left(\frac{K_1}{m_1 + m_2}\right)^{\frac{1}{2}} \Big/ \Omega, \qquad \omega_2 = \left(\frac{K_2}{m_2 r_2^2}\right)^{\frac{1}{2}} \Big/ \Omega. \tag{12}$$

The non-dimensional damping parameters are defined as

$$\gamma_1 = \frac{C_1}{m_1 + m_2} \Big/ \Omega, \qquad \gamma_2 = \frac{C_2}{m_2 r_2^2} \Big/ \Omega. \tag{13}$$

The forcing frequencies in (8) are

$$\Omega_1 = \Omega_\theta/\Omega, \qquad \Omega_2 = \Omega_r/\Omega. \tag{14}$$

Having non-dimensionalized the differential equations, we now proceed to scale them. This process inserts a small dimensionless parameter ε in the equations, $\varepsilon \ll 1$, which represents the order of nonlinearities and coupling. This step will be important for our perturbation solution. We shall choose ε so that we perturb off the linear equations for small ε. To begin with, we posit a change of variables such that

$$\theta_2 = \varepsilon\theta, \qquad \rho_1 = \varepsilon^n\rho, \qquad \theta_1 = \varepsilon^j\varphi, \qquad F_1 = \varepsilon^k f_1, \tag{15}$$

with n, j and k integers greater than or equal to one, the values of which are to be determined. Then we substitute equations $(15)_{1,2}$ into $(8)_{1,2}$ and expand the resulting equations using Taylor series for small ε. In particular, $\sin(\varepsilon\theta)$ and $\cos(\varepsilon\theta)$ are replaced by $\varepsilon\theta + \ldots$ and $1 - \ldots$, respectively. This leads to

$$\left.\begin{aligned} &\varepsilon^n\ddot{\rho} + \gamma_1\varepsilon^n\dot{\rho} + \omega_1^2\varepsilon^n\rho - m\varepsilon^2\theta\ddot{\theta} - m\varepsilon^2\dot{\theta}^2 - m\varepsilon^{j+1}\ddot{\varphi}\theta \\ &\qquad -2m\varepsilon^{j+1}\dot{\varphi}\dot{\theta} - \varepsilon^{n+2j}\rho\dot{\varphi}^2 - m\varepsilon^{2j}\dot{\varphi}^2 = \varepsilon^k f_1\omega_1^2\cos(\Omega_1\tau), \\ &\varepsilon\ddot{\theta} + \varepsilon\gamma_2\dot{\theta} + \varepsilon\omega_2^2\theta - \varepsilon^{n+1}\ddot{\rho}\theta + \varepsilon^{n+j}\dot{\rho}\dot{\varphi} + \varepsilon^{n+2j+1}\rho\dot{\varphi}^2\theta + 2\varepsilon^{n+j}\dot{\rho}\dot{\varphi} \\ &\qquad = -\varepsilon^j\ddot{\varphi}. \end{aligned}\right\} \tag{16}$$

At this point we require the linear terms to be of at least one order ε lower than the nonlinear terms. In equation $(16)_1$, comparing $\varepsilon^n\ddot{\rho}$, $m\varepsilon^2\theta\ddot{\theta}$ and $m\varepsilon^{j+1}\theta\ddot{\varphi}$ terms, we require the linear terms $\ddot{\rho}$ and ρ to be of lower order than the nonlinear terms $\theta\ddot{\theta}$ and $\theta\ddot{\varphi}$. This gives

$$n < 2, \qquad n < j + 1. \tag{17}$$

Similarly, for the forcing term to be of higher order than the linear terms, we must have

$$k \geqslant n. \tag{18}$$

Likewise, the nonlinear, parametric and forcing terms in $(16)_2$ must have higher order than the linear terms. This gives the following relations:

$$j \geqslant 1, \qquad n + 1 > 1, \tag{19a}$$

or

$$n > 0. \tag{19b}$$

Equation $(17)_1$ requires that $n = 1$ and $(17)_2$ is satisfied by $j = 1$. Then (18) becomes

$$k \geqslant 1. \tag{20}$$

The choice of k determines the magnitude of the translational excitation amplitude.

In order to purturb off from the undamped linear equations, we choose to scale the damping coefficients γ_1 and γ_2 as

$$\gamma_1 = \varepsilon\mu_1, \qquad \gamma_2 = \varepsilon\mu_2. \tag{21}$$

With these assumptions, the equations of motion take the following form:

$$\left.\begin{aligned} &\ddot{\rho} + \varepsilon\mu_1\dot{\rho} + \omega_1^2\rho - m\varepsilon(\theta\ddot{\theta} + \dot{\theta}^2) - m\varepsilon(\theta\ddot{\varphi} + 2\dot{\theta}\dot{\varphi}) - \varepsilon^2\rho\dot{\varphi}^2 \\ &\qquad = m\varepsilon\dot{\varphi}^2 + \varepsilon^{k-1}f_1\omega_1^2\cos(\Omega_1\tau), \\ &\ddot{\theta} + \varepsilon\mu_2\dot{\theta} + \omega_2^2\theta - \varepsilon\ddot{\rho}\theta + \varepsilon(\rho\ddot{\varphi} + 2\dot{\rho}\dot{\varphi}) = -\ddot{\varphi}, \end{aligned}\right\} \tag{22}$$

where

$$\varphi = F_2\sin(\Omega_2\tau). \tag{23}$$

The two-variable expansion-pertrubation method

When flexibility is introduced in the robot arm, study of the resonances becomes crucial. This is particularly important when the robot is required to perform the same task for various payloads of different sizes and weights, causing the natural frequencies of the system to vary for each payload. For example, if the payload is such that $\omega_1 \simeq 2\omega_2$ (for a two-degree-of-freedom system), then internal resonance must be considered. Moreover, we expect the usual case of forced resonance to occur at $\Omega_i \simeq \omega_i$. In such resonant cases, the response of the system becomes complicated and the robotic device may not perform the desired task. The goal of our perturbation analysis is to help us understand the dynamics of the system near internal or forced resonances in order to improve the design of the robotic device.

Using the two-variable expansion-perturbation method (Kevorkian and Cole, 1968; Nayfeh, 1973; Keith, 1983; Rand, 1985; Rand *et al.*, 1987), we replace the independent variable τ by two new variables, ξ and η, such that

$$\xi = \tau, \qquad \eta = \varepsilon\tau; \tag{24}$$

where ξ is just τ and η is a slow time variable. The idea of the method is to permit the dependent variables ρ and θ to depend explicitly on two time scales, ξ and η. For example, periodic steady-state behaviour will occur in ξ, while approach to steady state will occur in η.

Using the chain rule, we can rewrite the time derivatives of $r(\xi, \eta)$ and $\theta(\xi, \eta)$ as

$$\frac{d}{d\tau} = \alpha\frac{\partial}{\partial\xi} + \varepsilon\frac{\partial}{\partial\eta}, \qquad \frac{d^2}{d\tau^2} = \alpha^2\frac{\partial^2}{\partial\xi^2} + 2\alpha\varepsilon\frac{\partial^2}{\partial\xi\partial\eta} + O(\varepsilon^2). \tag{25}$$

We also expand ρ and θ as

$$\rho = \rho_0 + \varepsilon\rho_1 + O(\varepsilon^2), \qquad \theta = \theta_0 + \varepsilon\theta_1 + O(\varepsilon^2). \tag{26}$$

At this stage we are ready to analyse the equations of motion.

The forced resonance $\Omega_1 \simeq \omega_1$

Perturbation study of the forced system is of particular interest since, in practice, robotic devices must follow periodic tasks with a combination of forcing frequencies. For a two-degree-of-freedom mechanism, with Ω_1 and Ω_2 as the driving frequencies, a periodic task is defined by $\Omega_1 = p\Omega_2$ for some integer p.

Forced resonances include $\Omega_1 \simeq \omega_1$, $\Omega_2 \simeq \omega_2$, $\Omega_2 \simeq \omega_1 + \omega_2$, $\Omega_2 \simeq \omega_1 - \omega_2$ and $\Omega_2 \simeq \frac{1}{2}\omega_1$. In this paper we shall consider only $\Omega_1 \simeq \omega_1$. See (Golnaraghi, 1988) for analysis of other resonances. In the study of such resonances, we must distinguish between the case of internal resonance $\omega_1 \simeq 2\omega_2$ and the case of no internal resonance (that is, ω_1 is away from $2\omega_2$). For the internal-resonance case, we detune the resonance with the parameter σ_1 such that

$$\Omega_1 = \omega_1 + \varepsilon\sigma_1. \tag{27}$$

Let us now consider the case where $\Omega_1 \simeq \omega_1$. We choose $k = 1$ in (15) so that $F_1 = \varepsilon f_1$. For consistency of notation, we write $F_2 = f_2$.

Substituting (24) to (26) into (22) and collecting terms, we find the zeroth- and

first-order equations to be as follows. For order ε^0:

$$\rho_{0\xi\xi} + \omega_1^2\rho_0 = 0, \qquad \theta_{0\xi\xi} + \omega_2^2\theta_0 = \Omega_2^2 f_2 \sin(\Omega_2\xi); \tag{28}$$

for order ε:

$$\left.\begin{aligned}\rho_{1\xi\xi} + \omega_1^2\rho_1 = {} & -2\rho_{0\xi\eta} + m\theta_0\theta_{0\xi\xi} + m(\theta_{0\xi})^2 - \mu_1\rho_{0\xi} \\ & + 2\Omega_2 f_2 m\theta_{0\xi}\cos(\Omega_2\xi) - \Omega_2^2 f_2 m\theta_0 \sin(\Omega_2\xi) \\ & + \Omega_2^2 f_2^2 m\cos^2(\Omega_2\xi) + f_1\omega_1^2\cos(\Omega_1\xi), \\ \theta_{1\xi\xi} + \omega_2^2\theta_1 = {} & -2\theta_{0\xi\eta} - \mu_2\theta_{0\xi} - 2\Omega_2 f_2\rho_0\cos(\Omega_2\xi) + \Omega_2^2 f_2\rho_0\sin(\Omega_2\xi).\end{aligned}\right\} \tag{29}$$

Here the subscripts represent partial derivatives. The solutions of $(28)_{1,2}$ can be written in the form

$$\left.\begin{aligned}\rho_0 &= K_1(\eta)\sin(\omega_1\xi) + K_2(\eta)\cos(\omega_1\xi), \\ \theta_0 &= K_3(\eta)\sin(\omega_2\xi) + K_2(\eta)\cos(\omega_2\xi) + Q_1\sin(\Omega_2\xi),\end{aligned}\right\} \tag{30}$$

where

$$Q_1 = \frac{\Omega_2^2 f_2}{\omega_2^2 - \Omega_2^2}. \tag{31}$$

We now substitute $(30)_{1,2}$ into equations (29), suppressing the secular terms $\sin(\omega_1\xi)$ and $\cos(\omega_1\xi)$ in $(29)_1$, and $\sin(\omega_2\xi)$ and $\cos(\omega_2\xi)$ in $(29)_2$. Note that we have written

$$\begin{aligned}\cos(\Omega_1\xi) &= \cos(\omega_1 + \varepsilon\sigma_1\xi) = \cos(\omega_1\xi + \eta\sigma_1) \\ &= \cos(\omega_1)\cos(\sigma_1\eta) - \sin(\omega_1\xi)\sin(\sigma_1\eta).\end{aligned} \tag{32}$$

Due to the length of the expressions, we shall eliminate some of the intermediate steps. We shall consider two cases; namely, the *non-resonant* case when ω_1 is away from $2\omega_2$, and the *internal-resonant* case when $\omega_1 \simeq 2\omega_2$. In this work, the significance of resonance is the appearance of additional secular terms in the two-variable expansion method.

The non-resonant case

Before writing the solvability conditions, we introduce a polar transformation such that

$$K_1 = a_1\sin(\varphi_1), \quad K_2 = a_1\cos(\varphi_1), \quad K_3 = a_2\sin(\varphi_2), \quad K_4 = a_2\cos(\phi_2), \tag{33}$$

where a_n and φ_n are real functions of η. This enables us to obtain the secular-term equations in a more convenient form, namely

$$\left.\begin{aligned}a_{1\eta} &= -\frac{\mu_1}{2}a_1 + \frac{f_1\omega_1}{2}\sin(\psi), \\ a_{2\eta} &= -\frac{\mu_2}{2}a_2, \\ \psi_\eta &= \sigma_1 + \frac{f_1\omega_1}{2a_1}\cos(\psi),\end{aligned}\right\} \tag{34}$$

where

$$\psi = \sigma_1 \eta + \varphi_1, \qquad \varphi_2 = \text{constant}.$$

The equilibrium solution is obtained when each right-hand side in (34) is set equal to zero. So we will have

$$\left.\begin{aligned} a_1 &= \frac{f_1 \omega_1}{2(\sigma_1^2 + \mu_1^2/4)^{\frac{1}{2}}}, \\ a_2 &= 0, \\ \psi &= \tan^{-1} \frac{\mu_1}{2\sigma_1}. \end{aligned}\right\} \tag{36}$$

Stability analysis of (36), performed by linearizing equations (34) around the equilibrium values, shows that the the equilibrium solution is stable. Thus, the steady-state solutions for ρ and θ (that is, as $\tau \to \infty$) are

$$\left.\begin{aligned} \rho &= \frac{F_1 \omega_1 \varepsilon^{-1}}{2(\sigma_1^2 + \mu_1^2/4)^{\frac{1}{2}}} \cos(\Omega_1 \tau - \psi) + O(\varepsilon), \\ \theta &= \frac{F_2 \Omega_2^2}{\omega_2^2 - \Omega_2^2} \sin(\Omega_2 \tau) + O(\varepsilon). \end{aligned}\right\} \tag{37}$$

Therefore, the $O(\varepsilon)$ solution of the system is just that of the linear system.

The case of internal resonance ($\omega_1 \simeq 2\omega_2$)

This is the case when ω_1 is very close to $2\omega_2$. We introduce a detuning parameter σ_2 to show the nearness of the two frequencies. Hence,

$$\omega_1 = 2\omega_2 + \varepsilon \sigma_2. \tag{38}$$

As in the previous case, we switch to polar form using (33). Furthermore, in addition to (32) we write

$$\left.\begin{aligned} \cos(\omega_1 \xi) &= \cos(2\omega_2 \xi + \varepsilon \sigma_2 \xi) = \cos(2\omega_2 \xi + \eta \sigma_2) \\ &= \cos(2\omega_2 \xi) \cos(\sigma_2 \eta) - \sin(2\omega_2 \xi) \sin(\sigma_2 \eta), \\ \sin(\omega_1 \xi) &= \sin(2\omega_2 \xi + \varepsilon \sigma_2 \xi) = \sin(2\omega_2 \xi + \eta \sigma_2) \\ &= \cos(2\omega_2 \xi) \sin(\sigma_2 \eta) + \sin(2\omega_2 \xi) \cos(\sigma_2 \eta), \end{aligned}\right\} \tag{39}$$

Thus, the non-autonomous solvability equations, in polar form, are

$$\left.\begin{aligned} a_{1\eta} &= \frac{m\omega_2^2}{\omega_1} a_2^2 \sin(\psi_1) + \frac{f_1 \omega_1}{2} \sin(\psi_2) - \frac{\mu_1}{2} a_1, \\ a_{2\eta} &= -\frac{\omega_1^2}{4\omega_2} a_1 a_2 \sin(\psi_1) - \frac{\mu_1}{2} a_2, \\ \varphi_{1\eta} &= -\frac{m\omega_2^2}{2a_1\omega_1} a_2^2 \cos(\psi_1) + \frac{f_1 \omega_1}{2a_1} \cos(\psi_2), \\ \varphi_{2\eta} &= -\frac{\omega_1^2}{4\omega_2} a_1 \cos(\psi_1), \end{aligned}\right\} \tag{40}$$

where

$$\psi_1 = \eta\sigma_1 + \varphi_1, \qquad \psi_2 = \eta\sigma_2 + 2\varphi_2 - \varphi_1. \tag{41}$$

Eliminating φ_1 and φ_2 from equations (40), we obtain the following set of equations:

$$\left.\begin{aligned}
a_{1\eta} &= \frac{m\omega_2^2}{2\omega_1} a_2^2 \sin(\psi_2) + \frac{f_1\omega_1}{2} \sin(\psi_1) - \frac{\mu_1}{2} a_1, \\
a_{2\eta} &= -\frac{\omega_1^2}{4\omega_2} a_1 a_2 \sin(\psi_2) - \frac{\mu_1}{2} a_2, \\
\psi_{1\eta} &= -\frac{m\omega_2^2}{2a_1\omega_1} a_2^2 \cos(\psi_2) + \frac{f_1\omega_1}{a_1} \cos(\psi_1) + \sigma_1, \\
\psi_{2\eta} &= -\frac{\omega_1^2}{2\omega_2} a_1 \cos(\psi_{22}) + \frac{m\omega_2^2}{2a_1\omega_1} a_2^2 \cos(\psi_2) - \frac{f_1\omega_1}{2a_1} \cos(\psi_1) + \sigma_2.
\end{aligned}\right\} \tag{42}$$

There are two possibilities for the equilibrium solutions, $a_{i\eta} = \psi_{i\eta} = 0$, to (42). The first case is

$$\left.\begin{aligned}
&a_2 = 0, \qquad a_1 = \frac{f_1\omega_1}{2(\sigma_1^2 + \mu_1^2/4)^{\frac{1}{2}}}, \\
&\psi_1 = -\tan^{-1}\frac{\mu_1}{2\sigma_1}, \qquad \psi_2 = \text{arbitrary},
\end{aligned}\right\} \tag{43}$$

which implies that the $O(\varepsilon)$ solution is essentially that of the linear system, as follows:

$$\left.\begin{aligned}
\rho &= \frac{F_1\omega_1\varepsilon^{-1}}{2(\sigma_1^2 + \frac{1}{4}\mu_1^2)^{\frac{1}{2}}} \cos(\Omega_1\tau - \psi_1) + O(\varepsilon), \\
\theta &= \frac{F_2\Omega_2^2}{\omega_2^2 - \Omega_2^2} \sin(\Omega_2\tau) + O(\varepsilon).
\end{aligned}\right\} \tag{44}$$

The second case is

$$\left.\begin{aligned}
a_1 &= \frac{2\omega_2}{\omega_1^2}((\sigma_1 + \sigma_2)^2 + \mu_2^2)^{\frac{1}{2}}, \\
a_2 &= \frac{1}{\omega_2}\left[\frac{\Gamma_1 \pm (f_1^2\omega_1^6 - \Gamma_2^2)^{\frac{1}{2}}}{m\omega_1}\right]^{\frac{1}{2}}, \\
\psi_1 &= \tan^{-1}\frac{\mu_2 a_2^2\omega_2^3 + \frac{1}{2}\mu_1 a_1^2\omega_1^3}{m\omega_2^3 a_2^2(\sigma_1 + \sigma_2) - \omega_1^3\sigma_1 a_1^2}, \\
\psi_2 &= -\tan^{-1}\frac{\mu_2}{\sigma_1 + \sigma_2},
\end{aligned}\right\} \tag{45}$$

where

$$\Gamma_1 = (4\sigma_1(\sigma_1 + \sigma_2) - 2\mu_1\mu_2)\omega_2, \qquad \Gamma_2 = (2\mu_1(\sigma_1 + \sigma_2) + 4\mu_1\mu_2)\omega_2. \tag{46}$$

Hence, the steady state response for this case, with the use of equations (45), is

$$\left.\begin{aligned}\rho &= \frac{2\omega_2}{\omega_1^2}((\sigma_1+\sigma_2)^2+\mu_2^2)^{\frac{1}{2}}\cos(\Omega_1\tau-\psi_1)+O(\varepsilon),\\ \theta &= \frac{F_2\Omega_2^2}{\omega_2^2-\Omega_2^2}\sin(\Omega_2\tau)\\ &\quad+\frac{1}{\omega_2}\left[\frac{\Gamma_1\pm(F_1^2\varepsilon^{-1}\omega_1^6-\Gamma_2^2)^{\frac{1}{2}}}{m\omega_1}\right]^{\frac{1}{2}}\cos(\tfrac{1}{2}(\Omega_2\tau-\psi_2-\psi_1))+O(\varepsilon).\end{aligned}\right\}\quad(47)$$

Comparing the two possible solutions, (44) and (47), we can see that when internal resonance exists, the solution to θ has an extra term beyond that of the non-resonant solution. This implies that θ will be excited by half the frequency of translation Ω_1 in addition to the rotational forcing frequency Ω_2. From the solution to ρ, we see two major differences with respect to the non-resonant solution. First, the amplitude of the ρ mode is independent of the forcing amplitude f_1 (that is, saturation phenomenon). Secondly, the approximate solution for θ has an additional term at resonance.

In order to illustrate the system behaviour at resonance, we numerically integrate the governing equations for a_i and ψ_i (42) and compare the results with the solution of (43) and (45) which are the equations defining the steady-state values of the response amplitudes. For simplicity, in all cases we define $\Omega_1 = \Omega_2$.

Figure 3 illustrates the amplitudes of response as functions of the forcing amplitude f_1. In this case, $\sigma_2 = 0$ or $\omega_1 = 2\omega_2$ and $\sigma_1 = 0$ or $\Omega_1 = \Omega_2 = \omega_1$. As we

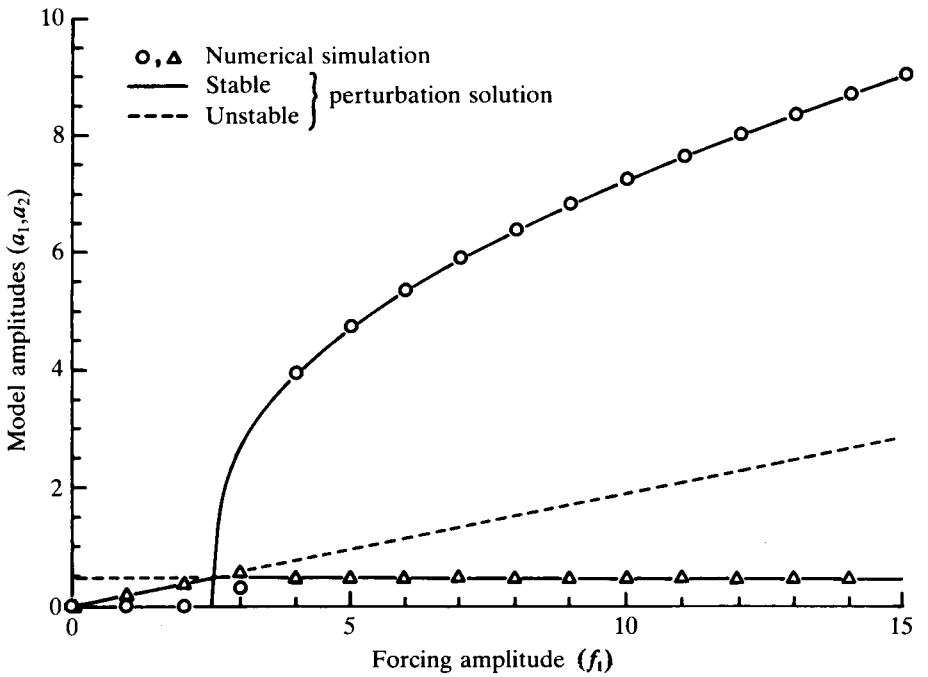

Fig. 3. Amplitudes of response versus the forcing amplitude f_1, showing perturbation solutions when $\sigma_2 = 0$, $\sigma_1 = 0$, and $\Omega_1 = \Omega_2$

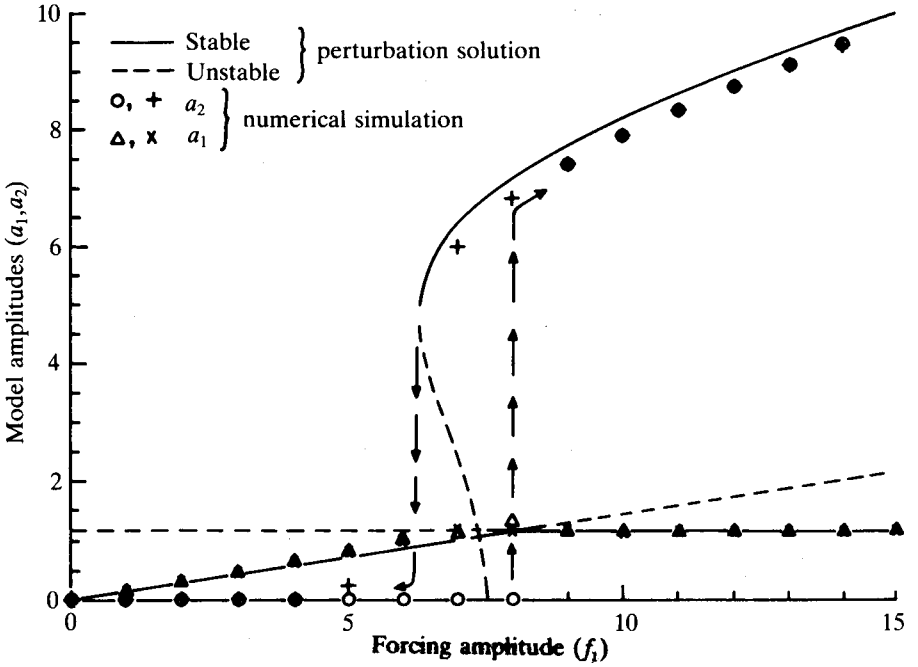

Fig. 4. Amplitudes of response versus the forcing amplitude f_1, showing perturbation solutions when $\sigma_2 = -0.87$, $\sigma_1 = 3.0$, and $\Omega_1 = \Omega_2$

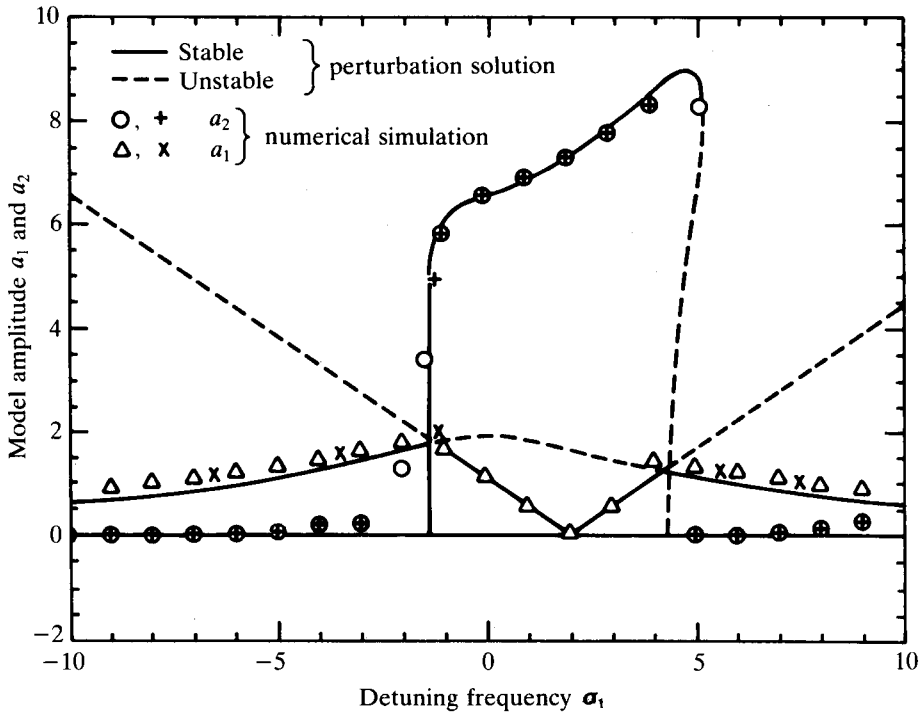

Fig. 5. Amplitude of response versus the detuning forcing frequency σ_1, showing perturbation solutions when $\sigma_2 = -2.0$, $f_1 = 10.0$, and $\Omega_1 = \Omega_2$

can see, there exists a critical value for f_1, obtained from (45):

$$f_1 = f_c = \frac{2\mu_1\mu_2}{\omega_1^6}\omega_2, \tag{48}$$

where for $f_1 < f_c$ the response is defined by equations (44), and for $f_1 > f_c$ the response follows (47). It should be noted that the solid lines in Fig. 3 define the stable solutions and the dotted lines define the unstable solutions. Stability analysis of the equilibrium solution was performed by linearizing equations (42) around the equilibrium values of a_1, a_2, ψ_1 and ψ_2, and obtaining the eigenvalues.

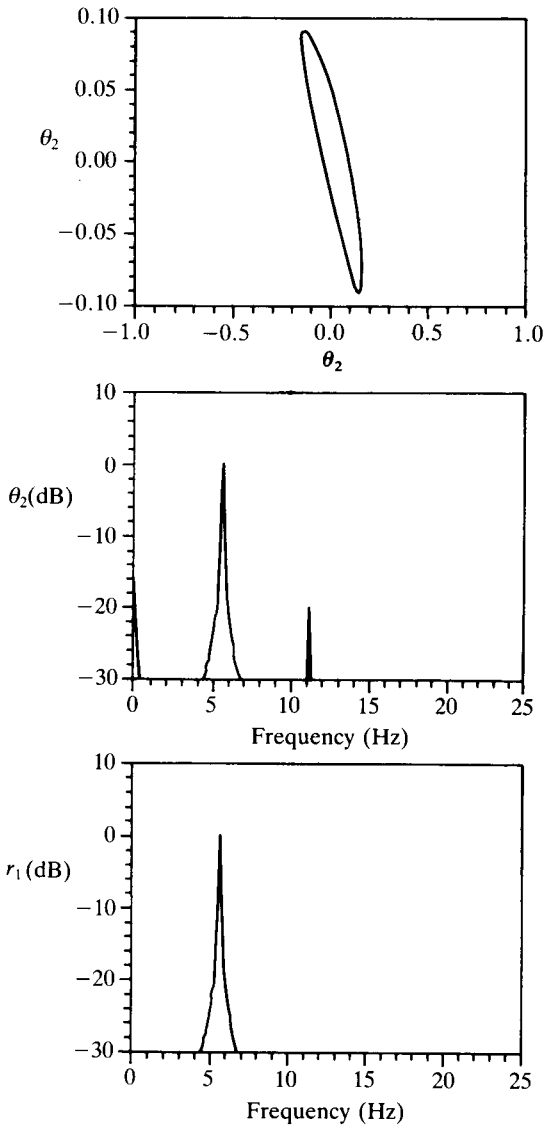

Fig. 6. Phase portrait and frequency spectra of the motion at $\Omega_r/\pi = 5.57$ Hz, prior to resonance

In contrast to Fig. 3 which involves parameters precisely at the resonance, we now consider detuning parameters (chosen to agree with experimental measurements). Figure 4 describes the amplitudes of response as the forcing amplitude f_1 varies for the perturbation solution. In this case, $\sigma_2 = -0.87$, $\sigma_2 = 3.0$ and $\Omega_1 = \Omega_2$. Here the jump occurs at two critical values of f_1. These values are defined by (45) as

$$f_1 = f_{c1} = \left|\frac{\Gamma_2}{\omega_1^3}\right|, \qquad f_1 = f_{c2} = \left|\frac{\Gamma_1^2 + \Gamma_2^2}{\omega_1^6}\right|, \tag{49}$$

where at $f_{c1} < f_1 < f_{c2}$, a_2 has one unstable and two stable solutions, and a_1 has two

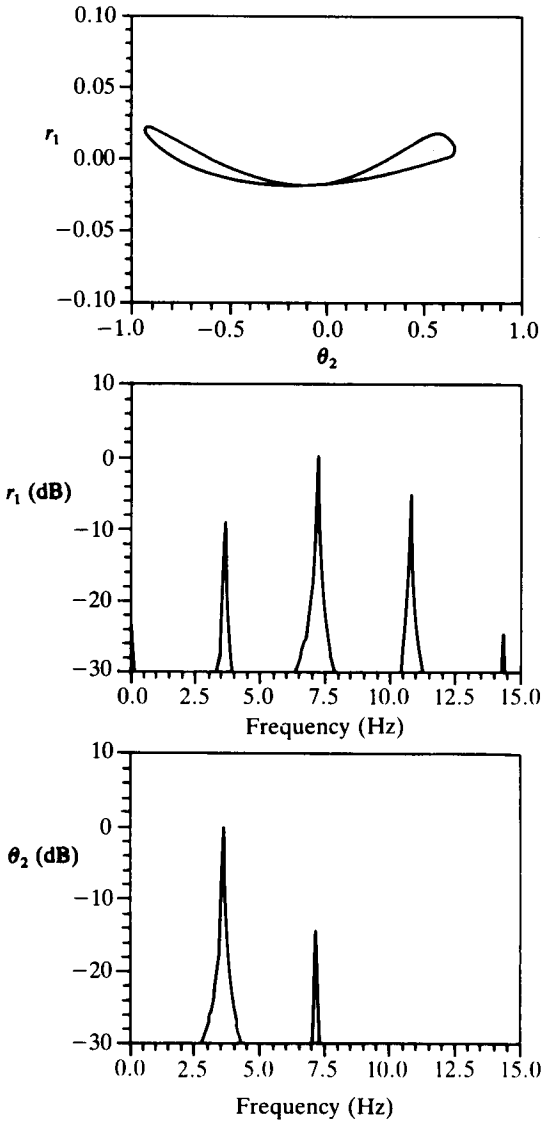

Fig. 7. Phase portrait and frequency spectra of the motion at $\Omega_r/\pi = 7.16$ Hz, during resonance

stable possible states. The values of a_1 and a_2 in this region depend upon the choice of the initial conditions.

Frequency response curves when $\sigma_2 = -2.0$, $f_1 = 10.0$ and $\Omega_1 = \Omega_2 = \omega_1 + \varepsilon\sigma_1$ are shown in Fig. 5. In this case, σ_1 corresponds to the detuning of the forcing frequency, so that when $\sigma_1 = 0$, the frequencies are related by $\Omega_1 = \Omega_2 = \omega_1$. Again, the jump and the stable and unstable solutions of the system are observed. The jump, however, occurs only in one side of the resonance curve, and that is due to the fact that $\sigma_2 \neq 0$; hence, the resonance curve is unsymmetric.

Figure 6 illustrates the phase portrait and the frequency spectra of the motion at $\Omega_r/\pi = 5.57$ Hz prior to resonance. Clearly, the response is following the driver. However, at $\Omega_r = 7.16$ Hz, the system is in resonance and exhibits a subharmonic response. The frequencies of this response are clearly shown in the frequency spectra of ρ and θ, shown in Fig. 7.

Experimental investigation of the forced resonance $\Omega_1 \simeq \omega_1$

In this section we consider the experimental study of the two-degree-of-freedom robotic mechanism, shown in Fig. 1. The flexible-arm robotic manipulator apparatus is shown in Fig. 8. The stainless steel arm had the dimensions $0.4 \times 2.54 \times 0.26$ cm. The gripper and the mass of payload were replaced by a single mass M_2 which was adjustable and varied from 0.5 to 1.4 kg. The bending deflection of the arm was measured through two strain gauges at the base of the beam. Constrained layer damping was provided through the application of 3M-SJ-2052X scotch damp (trade name) to the arm. The translational d.c. motor magnet assembly was represented by mass M_1 which travelled on a 30 cm guideway. The guideway consisted of two parallel stainless steel rods. Springs K_r were used to mechanically centre the position of M_1. An LVDT sensor determined the position of M_1 in volts, with zero volts showing the equilibrium position at the centre of the guideway. The translational input was sinusoidal and was provided by an HP 3300A function generator (trade name) and a Crown 300A Series II amplifier (trade name). A four bar linkage driving mechanism at the base converted the unidirectional rotation of a d.c. motor to oscillatory motion.

Both rotational and translational output signals, r_1 and θ_2, were amplified and filtered, for noise reduction, at 100 Hz using low-pass filters. These signals were observed and stored on a Nicolet digital oscilloscope (trade name). Continuous time traces in the phase planes (r_1, θ_2), $(r_1, \dot{r}_1)$, and $(\theta_2, \dot{\theta}_2)$ were recorded. Frequency spectra provided more accurate readings and resulted in a clearer understanding of system characteristics. Frequency power spectra of the position signals were obtained using HP 3562A Dynamic Signal Analyzer (trade name).

Existence of a jump phenomenon

As discussed earlier, the system with which we are concerned possesses quadratic nonlinearities arising from the kinematic terms such as inertia, Coriolis and centripetal accelerations. Furthermore, we found analytically that for our two-degree-of-freedom system possessing quadratic nonlinearities, interesting phenomena were predicted to occur when the natural frequencies were 2:1, such

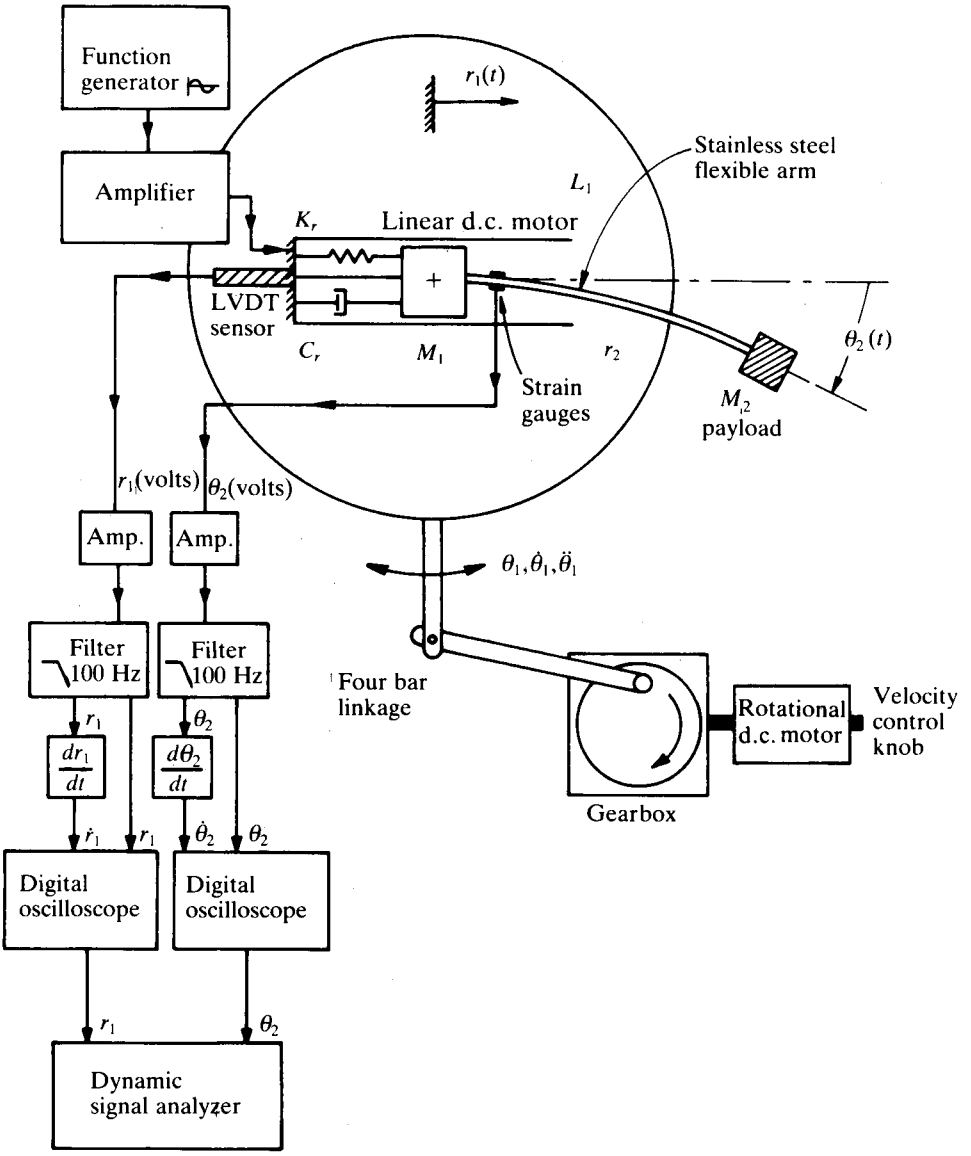

Fig. 8. Experimental set-up of the two-degree-of-freedom manipulator

Table 1. The system parameter values

K_1 (N/m)	K_2 (N·m)	M_1 (kg)	M_2 (kg)	$C_1\left(\frac{\text{N}}{\text{m.s}}\right)$	$C_2\left(\frac{\text{N}\cdot\text{m}}{\text{s}}\right)$	ω_r/π (Hz)	ω_θ/π (Hz)
3439.0	105.0	0.7	1.4	45.0	0.055	6.6	3.45

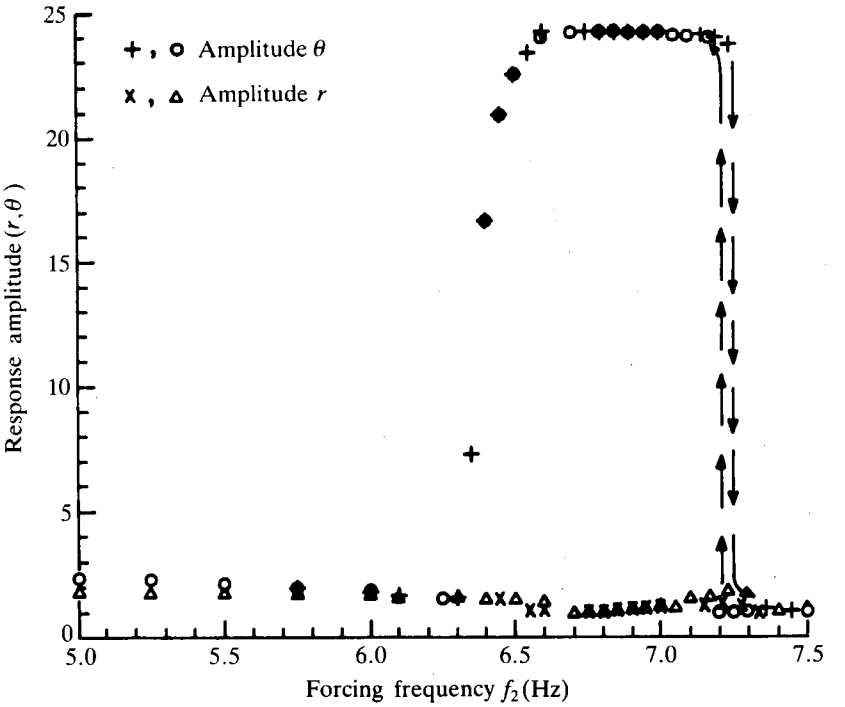

Fig. 9. Frequency response showing the primary resonance and the existence of a jump phenomenon

that $\omega_r \simeq 2\omega_\theta$. Moreover, we predicted that the case of forced resonance, when the frequency of excitation Ω_r was near the natural frequency ω_r, was particularly interesting.

In this section we choose the dimensions, weights and other parameters of the system as shown in Table 1, to induce a 2:1 relationship between the natural frequencies (that is, internal resonance $\omega_r \simeq 2\omega_\theta$). In addition, we have constrained the forcing frequency Ω_r to vary in the neighbourhoods of ω_r, in order to investigate the behaviour at the primary resonance. For constant forcing amplitudes F_r and F_θ, the frequency response of the system was obtained by incremental increase of $\Omega_r = \Omega_\theta$ with initial value $\Omega_r/\tau = 5.5$ Hz, as shown in Fig. 9. The r_1 and θ_2 samples taken while Ω_r increased were marked ○, △ and those collected when Ω_r decreased were marked ×, +. The diagram illustrates the steady-state responses and a jump phenomenon at $\Omega_r/\pi = 7.3$ Hz. The jump implies that the response is multivalued, and occurs only in one side of the curve and is not symmetric. In this case the natural frequencies were $\omega_r/\pi = 6.6$ and $\omega_\theta/\pi = 3.45$ Hz (that is, $\omega_r = 2\omega_\theta + \varepsilon\sigma$) and consequently the results lack symmetry. We observed the same phenomenon when Ω_r was fixed and the forcing amplitude increased. Figure 10 illustrates the case where $\Omega_r/\pi = 6.8$ Hz and the forcing amplitude F_1 varied from 0 to 5.0 volts.

The phase plot (θ_2, r_1) and the frequency spectra for θ_2 and r_1 when $\Omega_r/\pi = 6.8$ Hz, are shown in Fig. 11. A figure-eight in the (θ_2, r_1) phase plane represents the 2:1 ratio between the principle frequencies of r_1 and θ_2. As we

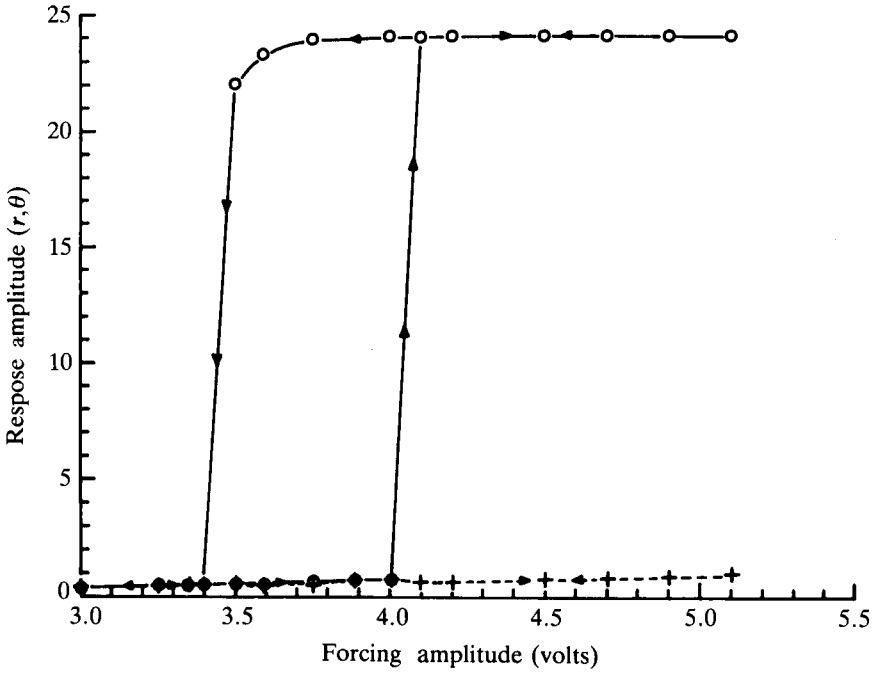

Fig. 10. Amplitude response showing the existence of a jump phenomenon when the forcing frequency $f_r = 6.8$ Hz

can see, at resonance both signals go through a subharmonic resonance, and the subharmonic frequency locks to exactly one-half of the forcing frequency.

Conclusions

In this paper we have performed analytical, numerical, and experimental investigation of the dynamics of a high-speed two-degree-of-freedom flexible-arm robotic device. Using a simple mathematical model, we studied the motion at

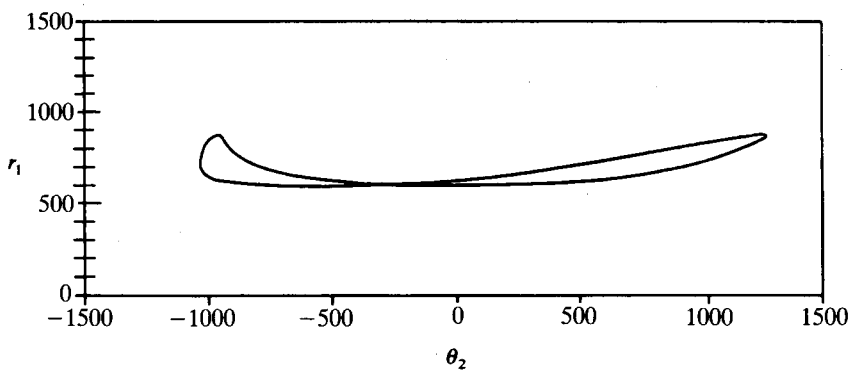

Fig. 11. The phase plots and the frequency power spectra of r_1 and θ_2 when $\Omega_r/\pi = f_r = 6.8$ Hz

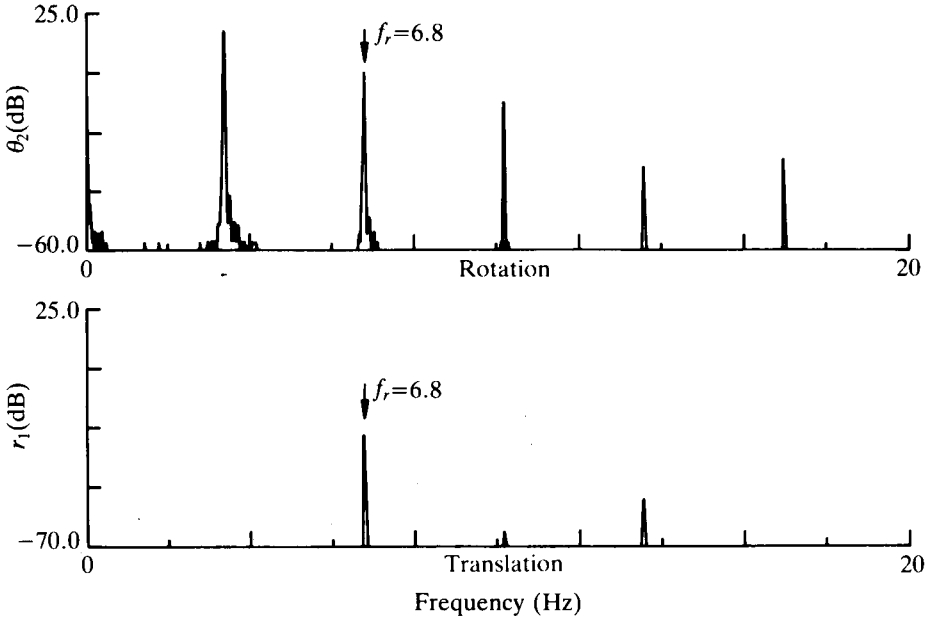

Fig. 11. Cont'd

resonance. We located all the possible resonances to the first order of approximation, and studied a case of forced resonance, that is, $\Omega_1 \simeq \omega_1$. Furthermore, we distinguished between the case of internal resonance, $\omega_1 \simeq 2\omega_2$, and the non-resonant case (that is, ω_1 is away from $2\omega_2$). Our studies showed that the solution for the non-resonant case was essentially that of the linear equation; whereas, at internal resonance interesting phenomena such as 'saturation' and 'jump' occur in the motion of the system. Finally, comparison of the perturbation and the numerical solutions with experimental results suggest that the mathematical model qualitatively predicts the motion of the physical system.

References

Chatraborty, T. and Rand, R. H. (1989) The transition from phase locking to drift in a system of two weakly coupled Van der Pol oscillators. *International Journal of Non-Linear Mechanics* to appear.

Cole, J. D. and Kevorkian, J. (1968) Uniformly valid asymptotic approximations for certain nonlinear differential equations. *Nonlinear Differential Equations and Nonlinear Mechanics* (eds J. P. LaSalle and S. Lefschetz; Academic Press, New York) 113–120.

Golnaraghi, M. F. (1988) Chaotic dynamics and control of nonlinear and flexible arm robotic devices. Ph.D. Dissertation, Cornell University.

Golnaraghi, M. F., Keith, W. K. and Moon, F. C. (1985) Stability analysis of a robotic mechanism using computer algebra. *Applications of Computer Algebra* (ed. R. Pavelle; Kluwer, Boston) 281–293.

Haddow, A. G., Barr, A. D. and Mook, D. T. (1984) *Theoretical and Experimental Study of Modal Interaction in a Two-Degree of Freedom Structure* (Academic Press, London) 451–473.

Keith, W. L. (1983) Phase locking and entrainment in two coupled limit cycle oscillators. Ph.D. Dissertation, Cornell University.

Keith, W. L. and Rand, R. H. (1973) 1:1 and 2:1 phase entrainment in a system of two coupled oscillators. *Journal of Mathematics and Biology* **20**, 133–152.

Nayfeh, A. H. (1973) *Perturbation Methods* (Wiley, New York).

Nayfeh, A. H. and Mook, D. T. (1979) *Nonlinear Oscillations* (Wiley, New York).

Rand, R. H. (1984). *Computer Algebra in Applied Mathematics: An Introduction to* MACSYMA (Pitman, Boston).

Rand, R. H. and Armbruster, D. A. (1987) *Perturbation Methods, Bifurcation Theory and Computer Algebra* (Springer, New York).

Storti, D. W. and Rand, R. H. (1982) Dynamics of two strongly coupled Van der Pol oscillators. *International Journal of Nonlinear Dynamics* **17**, 143–152.

Stupnicka, W. (1969) On the phenomennon of the combination type resonance in nonlinear two-degree of freedom systems. *International Journal of Non-Linear Mechanics* **4**, 335–359.

Stupnicka, W. (1974) On the phenomenon of the almost-periodic resonances in nonlinear vibrating systems with many degrees of freedom. *Nonlinear Vibration Problems* (Zagadnienia Drgan Nieliniowych) 221–231.

Stupnicka, W. and Bajkowski, J. (1980) Multi-harmonic response in the regions of instability of harmonic solution in multi-degree of freedom nonlinear systems. *International Journal of Non-Linear Mechanics* **15**, 1–11.

Van Dooren, R. (1971) Combination tones of summed type in a nonlinear damped vibratory system with two-degrees of freedom. *International Journal of Non-Linear Mechanics* **6**, 237–254.

Van Dooren, R. (1972) Forced oscillations in coupled Duffing equations by an analytical method of varying amplitudes and phase angles. *Koninklijke Vlaamse Academie van Belgie* **34**, 2.

Van Dooren, R. (1973) Differential tones in a damped mechanical system with quadratic and cubic nonlinearities. *International Journal of Non-Linear Mechanics* **8**, 575–583.

(Received October 1988)